ISSN : 2321-9416

Indo - American Journal of Mechanical Engineering

www.iajme.org

Email : iajme.editor@gmail.com or editor@iajme.org

Indo-American Journal of Mechanical Engineering

ISSN 2321–9416www.iajme.org
Vol 11, Issue 3,july 2023

Microstructure and mechanical properties of pure titanium models fabricated by selective laser melting

E C Santos1*, K Osakada1 , M Shiomi1 , Y Kitamura1

Abstract: Three-dimensional titanium models are created using the selective laser melting technique and a neodymium-doped yttrium aluminum garnet (Nd:YAG) pulsed laser, and then their pore structure, hardness, and mechanical characteristics are studied. Pore structure is shown to be sensitive to peak power, scan speed, and hatching pitch in both optical and scanning electron micrographs. Compared to wrought material (125-160 HV), the Vickers hardness of laser-formed specimens is roughly 240 HV (0.2 kgf). X-ray photoelectron spectroscopy (XPS) depth profiling reveals oxygen pick-up during laser shaping of the titanium prototype in an argon-filled, closed chamber. Titanium models were produced by varying the hatching pitch and laser power, and their fatigue strength was evaluated. Reduced hatching pitch or hot isostatic pressing (HIP) may increase the fatigue strength of the as-formed models. After HIP, the fatigue strength of the specimens is on par with that of the wrought material.

Keywords: Titanium, Microstructure, Microporosity, Selective Laser Melting, Mechanical Properties

1 INTRODUCTION

It seems that low-volume production runs of metal components may be handled well by rapid manufacturing (RM). Rapid prototyping (RP) methods and layer manufacturing techniques (LMT) are still not widely used for RM because to issues with the strength, surface roughness, and dimensional accuracy of the created models [1-3]. LMT has a lot of potential in the medical field. Prosthetics and implants have a high total cost due to the large number of unique parts required for each patient. The geometric information required for the production of the three-dimensional solid model can be acquired using three-dimensional scanning techniques like computerized axial tomography (CAT) and magnetic resonance imaging (MRI), and the final models can be produced using RP techniques like selective laser melting (SLM), selective laser sintering (SLS), and laser engineered net shaping (LENS). Medical components made from laser-formed parts often need further processing to achieve the required level of precision. One benefit-benefit of LMT is that it can produce components with tunable porosity by adjusting processing settings. One kind of RM technique that makes use of metal powder directly is called selective laser melting. Metal powders are fused in the focus zone of a high-energy laser beam, creating the desired component form in an automated, near-net-shape process that starts with CAD data. The SLM technique does not need the removal of any binders and may, in principle, employ any castable materials; nevertheless, it does require the precise selection of forming conditions to ensure proper functioning.

F Abe2 1 Division of Mechanical Science, Graduate School of Engineering Science, Osaka University, Osaka, Japan 2 Institute for Structural and Engineering Materials, National Institute of Advanced Industrial Science and Technology, Nagoya, Japan

Residual strains or fractures may form as a result of laser melting because to the strong temperature gradient caused by fast solidification. Annealing and hot isostatic pressing are two heat treatments that may enhance the final characteristics of the components by reducing stress and densifying them completely, respectively [4].
Titanium's high strength-to-weight ratio, corrosion resistance, and biocompatibility make it a desirable material. Titanium has these properties, thus it can be used to produce prosthetics and implants [5, 6].
Titanium is difficult to laser process because of the metal's strong reactivity to interstitial elements including oxygen, carbon, nitrogen, and hydrogen while in the molten form. SLM models of titanium demonstrate that the density of the specimens is more than scan speed and peak power have a little influence on the material's tensile strength, and the material's impact strength and fatigue strength are likewise quite modest [7-9]. In this study, we examine the effects of varying the peak power, scan speed, and hatching pitch of a pulsed neodymium-doped yttrium aluminum (Nd:YAG) laser on the pore structure and fatigue strength of pure grade 1 titanium powder. In order to learn more about the pore structure, scientists used both optical and scanning electron microscopes. Square bars with a variety of finishes underwent a torsional fatigue test. In order to increase the specimens' fatigue strength, heat treatments including annealing and hot isostatic pressing (HIP) were used.

1 EXPERIMENTAL PROCEDURES

The selective laser melting setup is shown in Figure 1. The highest peak power of the Nd:YAG laser employed was 3 kW, with an average power of 50 W. Due to the high irradiance (W/cm2) of the pulsed laser, powder may be effectively melted with a minimal heat-affected zone (HAZ) in the solidified portion provided the right settings are used. Furthermore, Nd:YAG lasers seem to be more suited than CO2 lasers for material processing when melting is involved [10, 11]. This is because metals have a higher absorptivity to short wavelength.
The optical fiber channels the laser's light, and its narrow, 0.8-mm beam hits the powder bed with pinpoint accuracy. The laser head is mounted on an x-y table that moves in response to computer commands. An optical laser travels along the
layers of solidified titanium powder placed on a steel substrate. The substrate is fastened to a piston that moves in the z direction down by a thickness of one layer, or 0.1 mm. To reduce the amount of oxygen and nitrogen absorbed, the procedure is performed in an enclosed chamber with constant argon flushing.
Titanium powder, grade 1, spherical (TILOP 45) was purchased from Sumitomo Sitix Inc. Table 1 displays the results of the powder's chemical analysis. The quantity of non-powder components in the powder was negligible. Particles were less than 45 millimeters in size, with an average size of 25 millimeters.
The 'x and y' scanning approach shown in Figure 2 is used to create the 3D models. The cross-section's outline is scanned first. Scanning occurs in both the x and y axes, but only for the odd layers (1, 3, 5, etc.). Layers 2, 4, 6, etc. are simply scanned at their edges since they are even. Layer 1 involves scanning in the x direction whereas layer 2 focuses only on the outline, layer 3 on the y, and finally layer 4 on the outline alone. This back-and-forth scanning process is continued until the final 3D object is created. This scanning technique shortens the building time because the even layers are not scanned in the x or y directions; instead, only the outline is scanned. This decreases the intercon- nected porosity between the layers and the anisotropy of the mechanical properties of the models (compared with one-directional scanning).
For the purpose of studying pore structure and taking hardness readings, cubes of 10 mm in length, blocks of 5 mm6 15 mm6 15 mm, and blocks of 2 mm610 mm6 10 mm were constructed. The fatigue tests were conducted on 53 mm square bars.

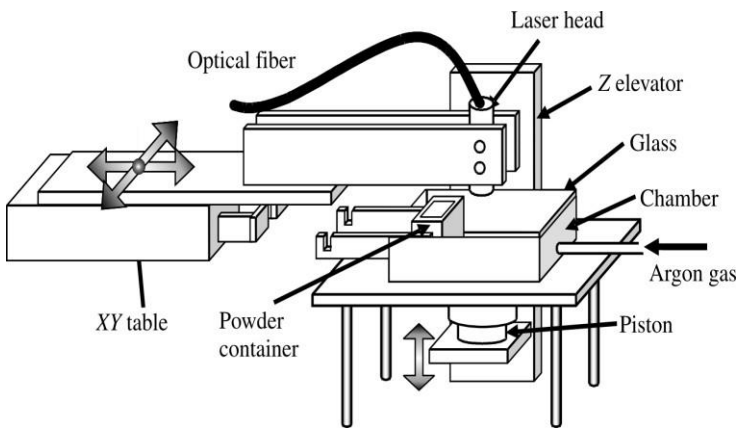

Fig. 1 Selective laser melting process

Table 1 Chemical composition of commercial pure titanium powder grade 1 TILOP 45 wt %

Oxygen	Nitrogen	Carbon	Iron	Hydrogen	Titanium
0.12	0.009	0.008	0.032	0.005	Balance

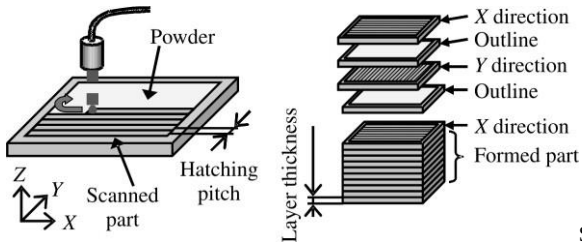

Source: Inspection Certificate, Sumitomo Sitix, Inc., Amagasaki, Japan Fig. 2 Scanning strategy

cross-section of 7 mm67 mm and 6 mm66 mm. The scan speed (v) and the peak power (P) were changed from 2 to 16 mm/s and from 0.5 to 1 kW respectively. The average power (P_{av}) and the frequency (f) were kept at 50 W and 50 Hz. The hatching pitch (h_p) was varied from 0.2 to 0.75 mm.

Two, the pore structure and the hardnessin peak powers of 0.5, 0.75, and 1 kW, the pore shape in the center of the produced cubes is shown in Figure 3. As the peak power rises, the crack-like pores transform into smooth, spherical ones. The mechanical characteristics of the models are impaired by the presence of the crack-like pores, which act as stress concentrators [12]. Optical micrograph of a specimen showing the results of employing varied scan speeds every 2-3 mm in the building direction (z) to create a cube with a cross-section of 5 mm615 mm and a height of 15 mm (Fig. 4). At scan rates of 4, 6, and 8 mm/s, the building-oriented cross-section of the specimen generated at these speeds reveals high density. When the scan speed is very fast, the porosity rises, and certain powder particles are not melted completely. significant-speed photography [7] revealed that the powder vaporized at a very slow rate of 2 mm/s, indicating a significant porosity. SEM images of the samples taken in the layer's center (XY plane) at 6 and 16 mm/s and with hatching pitches of 0.4 and 0.2 mm are shown in Figure 5. When making high-density components, the hatching pitch becomes smaller as the scan speed goes up. Hatching pitches of 0.4 mm for scan speeds of 6 mm/s and 0.2 mm for scan rates of 16 mm/s are recommended when the peak power is 1 kW, for example [13]. If you use the right values for your parameters (such hp = 0.2 mm and v = 16 mm/s), the density may go up to 98%.The results of varying the scan rate and peak power on the hardness are shown in Figure 6. At 4 mm/s and 1 kW of peak power, the average hardness is around 255 HV, whereas at 16 mm/s and 1 kW of peak power, it is approximately 218 HV. Wrought titanium grade 1 may have a hardness anywhere from 125 to 160 HV, depending on the presence of interstitial elements and the thermomechanical treatment it receives [14]. Picking up oxygen is a possible source of the increased hardness. X-ray photoelectron spectroscopy (XPS) depth profiling is used to assess the extent to which oxygen content has increased as a result of laser processing. MgKa radiation was used as the excitation source, and argon ion sputtering was accomplished (at 30 second intervals) under 4 keV of applied voltage for a total of 4.5 minutes. Hardness rises from 235 HV at 0.25 kW peak power to 265 HV at 2 kW peak power when the scan speed is held constant at 6 mm/s. The XPS profiles of the 1 kW (245 HV, 0.2 kgf) and 2 kW (Figure 7) specimens are shown.

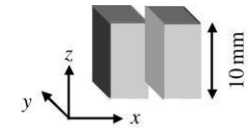

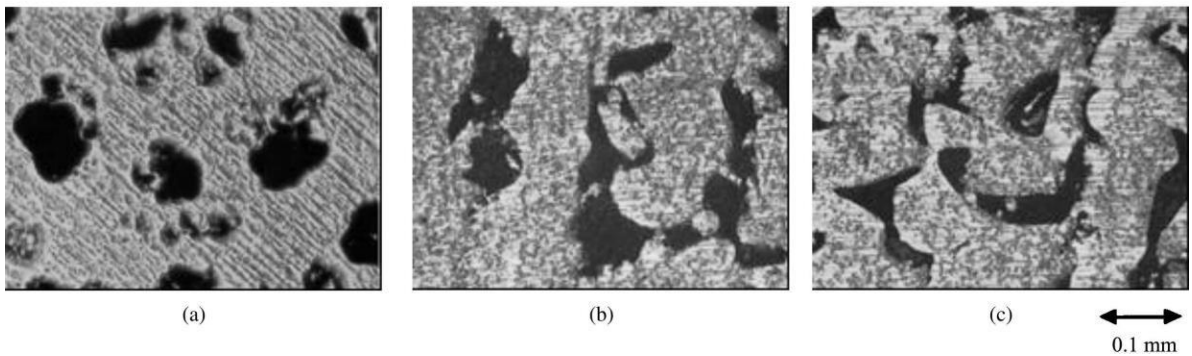

Fig. 3 Influence of the peak power on the pore shape: (a) $P = 1$ kW, (b) $P = 0.75$ kW and (c) $P = 0.5$ kW (P

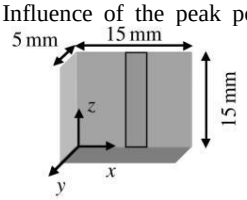

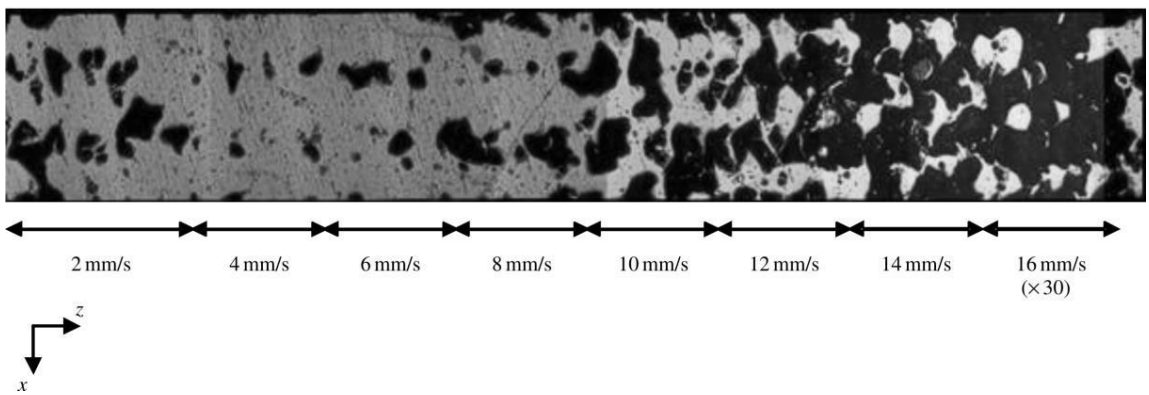

$_{av} = 50$ W, $f = 50$ Hz, $v = 6$ mm/s and $h_p = 0.75$ mm)

Fig. 4 Influence of the scan speed on the porosity ($P_{av} = 50$ W, $P = 1$ kW, $f = 50$ Hz and $h_p = 0.75$ mm)

Fig. 5 Influence of the hatching pitch on the porosity: (a) v = 6 mm/s, h_p = 0.75 mm; (b) v = 6 mm/s, h_p = 0.4 mm; (c) v = 16 mm/s, h_p = 0.75 mm; (d) v = 16 mm/s, h_p = 0.2 mm (P_{av} = 50 W, P = 1 kW and f = 50 Hz)

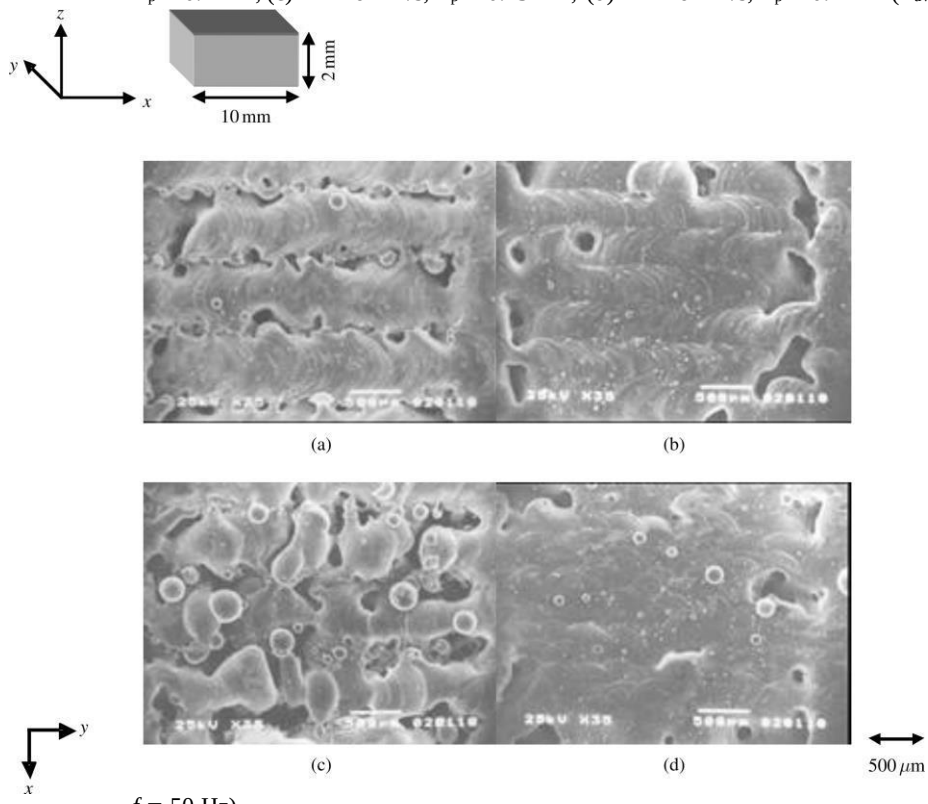

The peak areas give good qualitative information on the oxygen, carbon and titanium atomic concentration. Comparing the peak areas, it is possible to see that the specimen formed at a peak power of 2 kW has a higher

amount of oxygen. At a high peak power, the power density increases and the HAZ becomes large, which decreases the cooling rate. Therefore the amount of oxygen pick-up increases as the peak power increases.

ADVANTAGE NO. 2: FATIGUE

Because the surface layers of the metal are most strained during alternating bending or twisting, torsional or bending testing is superior than axial testing for evaluating the impact of surface condition. Torsional testing also has less issues with misalignment-related fatigue strength variation [15]. The bars utilized have a maximum 7 mm cross section and are 53 mm in length as test specimens. Both as-formed (immediately after laser processing) and machined (machining of 0.2 mm each side, grinding by 600-grit SiC paper, and polishing by alumina 1 mm) surface states are shown in the samples. Torsion stress and sample locations are shown in Figure 8. Figure 9 is a scanning electron micrograph showing the surface condition of the specimens towards their midpoint. This sintered

Figure 8b shows powder adhered to the edges of the specimen.

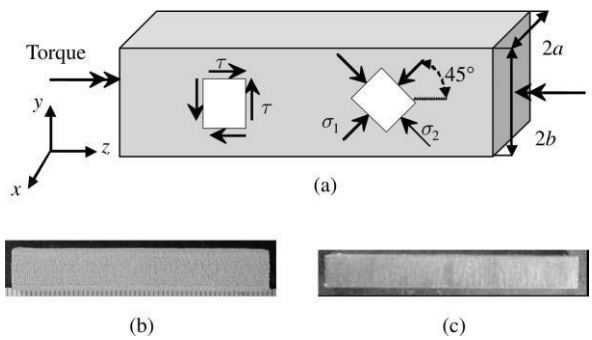

Fig. 8 Torsional fatigue test: (a) stress field during torsion test, (b) as-formed specimen (each division is 1 mm) and (c) machined

specimen (P_{av} = 50 W, P = 1 kW, f = 50 Hz and v = 6 mm/s)

calculated using the following equations [16]:

$$16a \sum (-1)^{(n-1)/2} \sin a_n x \cosh a_n y$$

and the shape parameter b = 0.141 for a square bar ($a = b$). The stress is higher in the middle of each side of the bar and is zero at the corners. The fatigue cycles are carried out at a fully reversed mode (stress ratio R = — 1) and the frequency of the machine is 33 Hz. The specimens were formed at peak powers of 0.5, 0.75 and 1 kW. The scan speed was 6 mm/s and hatching pitches of 0.75 and 0.4 mm were used.

The machined specimens built at a hatching pitch of 0.75 mm were submitted to heat treatment of annealing for stress relieving and HIP for densification. Annealing was done at a temperature of 750 8C, HIP was carried out at a temperature of 850 8C and pressure of 101 MPa in argon atmosphere and the specimens were kept for 1 h at the treatment temperatures.

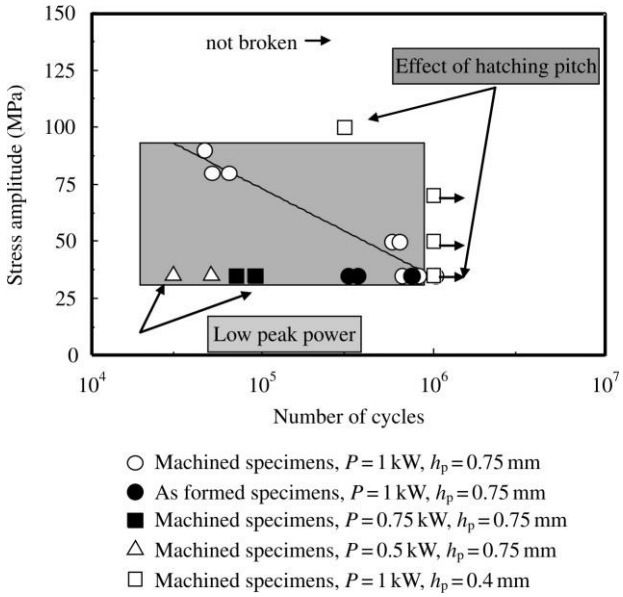

Fig. 10 Fatigue strength results of the laser-formed specimens (P_{av} = 50 W, f = 50 Hz and v = 6 mm/s)

2 CONCLUSIONS AND RECOMMENDATIONS

Figure 10 displays the stress amplitude-dependent number of cycles before failure for stress levels between 35 and 100 MPa. When the hatching pitch is 0.75 mm and the peak power is less than 1 kW (as shown by & and), the specimens are brittle and break before 105 cycles. At 1, 0.75, and 0.5 kW, the specimens had densities of 96%, 94%, and 94%, respectively. A strong effect of the crack-like pore shape and of the poor metallurgical connection between the layers on the fatigue strength is suggested by the low number of cycles before fracture at peak powers below 1 kW. As illustrated in Fig. 3, when peak power was reduced, spherical pores transformed into crack-like pores. Furthermore, the laser's intensity must be great enough to melt the powder and some of the preceding layer so that they can bind metallurgically well. Since peak power falls, so does the metallurgical connection between the layers.

Researchers are looking at the possibility of using implants with roughened surfaces or porous coatings to improve osseo-integration with bone [5]. When cement bonds to the porous covering, or when bone tissue grows into the coating, osseointegration is enhanced [5, 6]. Plasma spraying is often used as a post-processing step to generate porous coatings on implants. Traditional methods of applying porous coatings result in higher temperatures, which may generate significant grain development and notch effects, weakening the coating's fatigue resistance. Some studies have shown that conventional porous-coated titanium implants have a fatigue strength of 1/3 that of an uncoated implant [6].

The powder residue on the as-formed samples may be thought of as a porous covering. The sintered powder on the sample's surface is magnified in Figure 9b. The fatigue strength dropped very little as a consequence of this porous covering. Machined specimens were predicted to withstand more cycles before cracking than as-formed specimens because they had reduced surface roughness and fewer flaws (voids). Because the coating is produced during the building up of the specimens in the SLM process, the as-formed specimens (d) did not show a significant reduction in the number of cycles before fracturing when compared to the conventional machined specimens (s) for the stress of 35 MPa. Due to increased density and stronger metallurgical bonding between the scan tracks, specimens made with a hatching pitch of 0.4 mm (&) have a substantially greater fatigue strength than those generated with a hatching pitch of 0.75 mm.

The increase in fatigue strength following heat treatment is seen in Figure 11. Softening up (a little)

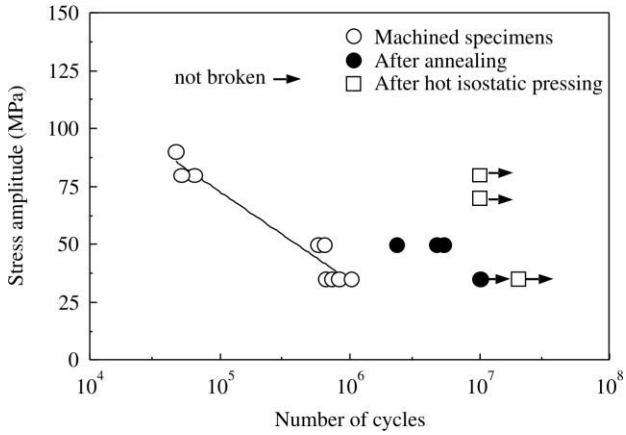

Fig. 11 Fatigue stre

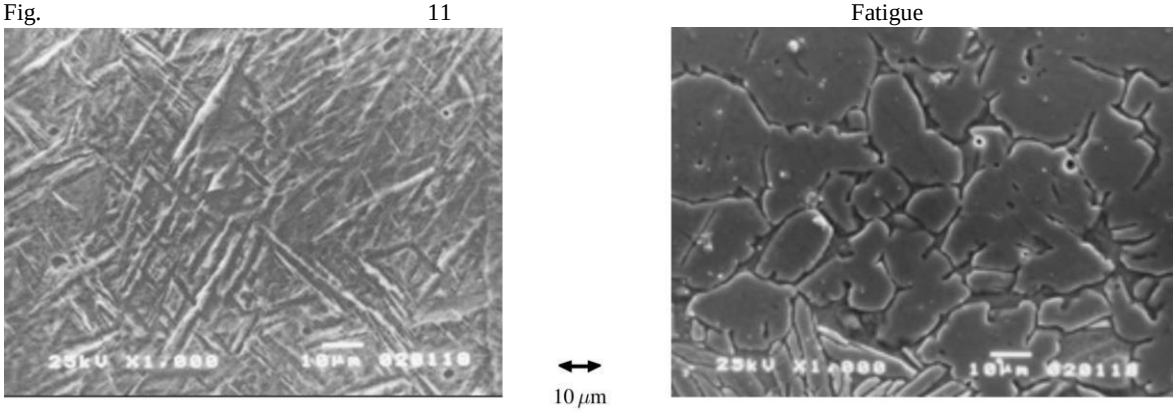

(a) (b)

ngth results of the heat-treated specimens (P_{av} = 50 W, f = 50 Hz, P = 1 kW, v = 6 mm/s and h_p = 0.75 mm)

Fig. 12 Microstructure of the specimens: (a) acicular martensitic before HIP, HV = 245; (b) equiaxed structure after HIP, HV = 220

reduces residual stresses in laser-formed objects, which improves their fatigue resistance. The fatigue strength is greatly enhanced and the density is brought close to 100% after HIP.

Sections of fatigue samples' microstructures before and after HIP are shown in Figure 12. As-formed specimens have an acicular martensitic microstructure because to the strong temperature gradient. After HIP, the specimens' microstructure is made up of grains that are now alpha equiaxed. The specimens' torsional fatigue strength after HIP (90-120 MPa to 106 cycles) is sufficient for dental implants and is equivalent to that of the wrought material (100-150 MPa for 106 cycles).

2 CONCLUSIONS

Laser parameters and forming circumstances' effects on part pore structure and fatigue strength were investigated, and various processing parameters and heat treatment were used to increase the fatigue strength of the laser-formed components. The key findings are:

First, in every scenario, the density is more than 92% after laser processing. Altering the forming parameters (scan pitch or layer thickness) or using hot isostatic pressing may improve the density to as high as 98%.

Laser processing increases the Vickers hardness beyond that of wrought titanium. The absorption of oxygen is to blame for the subsequent hardening.

3 The number of cycles that the machined specimens can tolerate before cracking is much greater. There is a need for more testing to determine the extent to which as-formed specimens lose fatigue strength when compared to their regular machined counterparts. The as-formed state may be seen as a coated component, with the added benefit of the coating being created in the forming process. Fourth, hot isostatic pressing after hatching with a big hatching pitch (say, hp = 0.75 mm for v = 6 mm/s) or a small hatching pitch (say, hp = 0.4 mm for v = 6 mm/s) may both result in a high fatigue strength.

REFERENCES

Laser Induced Materials and Processes for Rapid Prototyping, 2001 (Kluwer, Massachusetts) 1 Lu, L., Fuh, J. Y. H., and Wong, Y. S.

2 Surface roughness increase of indirect SLS metal components by laser surface polishing. Ramos, J. A.; Murphy, J.; Wood, K.; Bourell, D. L.; Beaman, J. J. Originally published in August 2001 as pages 28–38 in the proceedings of the 12th Solid Freeform Fabrication Symposium held at the University of Texas in Austin.

3 Report on the State of Rapid Prototyping and Tooling Worldwide: 2000 (Wholers Associates Inc., Colorado). Wohlers, T.

4 Das, S., Wohlert, M., Beaman, J. J., & Bourell, D. L. Selective laser sintering/hot isostatic pressing: fabrication of metal components. To wit: J. Metals, 50(12):17-20 (1998).

5 Brunette, David M., Peter Tengval, Michael Textor, and Peter Thomsen. Therapeutic titanium. Engineering Biological Responses and Medical Applications, in Material Science, Surface Science, 2001 (Springer, Berlin).

6 Medical uses of titanium and titanium alloys. J. E. Lemons and S. A. Brown. May 1996, ASTM PCN 04-012720-54, STP 1272, The Material and Biological Issues

Located in the city of Brotherly Love (Philadelphia), the American Society for Testing and Materials.

7 Citation: Abe, F., Santos, E. C., Osakada, K., & Shiomi, M. The effect of forming circumstances in selective laser melting fast prototyping of titanium. The Proceedings of the Institution of Mechanical Engineers, Volume 217, Issue C1, March 2003, Pages 119-126.

8 Mechanical characteristics of titanium models produced using selective laser melting. Santos, E., M. Shiomi, K. Osakada, and F. Abe. 2002 University of Texas at Austin Solid Freeform Symposium.

9 Shiomi, M., Osakada, K., Kitamura, Y., Santos, E., Abe, F., and Kitamura, Y. Titanium is being processed using selective laser melting for therapeutic applications. Malmoe, Sweden, November 1-2, 2000, site of the Rapid Prototyping and Manufacturing Conference and Exhibition.

10 Among the authors are J. P. Kruth, J. Bonse, S. Oorts, Ph. Hespel, L. Froyen, and T. Laoui. Selective laser sintering of metal powders: a comparison of Nd:YAG and CO2 lasers. In PHOTOMEC'99-ETE'99 Proceedings

Pages. 165-173 in Proceedings of the European Workshop, Liege, Belgium, 25-26 November 1999.

In 1997, Academic Press in New York published the second edition of Ready's Industrial Applications of Lasers1.

Second edition of Powder Metallurgy Science by R. M. German (Metal Powder Industries Federation, Princeton, NJ, 1994).

Three Santos, E. C. Selective laser melting in the processing of pure titanium. Research paper written for the Master's program in Engineering Science at Osaka University (Japan).

4 Mechanical characteristics of commercial grade titanium as affected by oxygen and hydrogen. Wasz ML, Brotzen FR, McLellan RB, Griffin AJ. Materials Research Bulletin 41 (1996):1-11.

5 Fatigue Resistance, by P. Ye. Kravchenko (O. M. Blunn, N. L. Day, translators), 1964 (Pergamon, Oxford).

6 S. Timonshenko and J. N. Goodier, "Theory of Elasticity," Third Edition, 1970, McGraw-Hill, Singapore, Engineering Mechanics Series.